# Detection of Sulfur Dioxide by Broadband Cavity Enhanced Absorption Spectroscopy (BBCEAS)

Ryan Thalman[1] and Jaron C. Hansen[2]

[1]Department of Chemistry, Snow College, Richfield, UT, USA
[2]Deparment of Chemistry and Biochemistry, Brigham Young, University, Provo, UT, USA

**Correspondence:** Ryan Thalman (ryan.thalman@snow.edu)

**Abstract.** Sulfur dioxide ($SO_2$) is an important precursor for formation of atmospheric sulfate aerosol and acid rain. We present an instrument using Broad Band Cavity Enhanced Absorption Spectroscopy (BBCEAS) for the measurement of $SO_2$ with a minimum limit of detection of 0.6 ppbv using the spectral range 305.5 – 312 nm and an averaging time of 60 seconds. The instrument consists of high reflectivity mirrors (0.9984 at 310 nm) and a deep UV light source. The effective absorption path length of the instrument is 610 m in a 0.957 m base length. Published reference absorption cross-sections were used to fit and retrieve the $SO_2$ concentrations and were compared to a diluted standard for $SO_2$. The comparison was well correlated, $R^2$ = 0.9985 with a correlation slope of 1.01.

## 1 Introduction

Sulfur dioxide ($SO_2$) is a precursor to formation of atmospheric sulfate aerosol and acid rain (Schwartz, 1987). $SO_2$ is emitted naturally through volcanic eruption (Holasek et al., 1996), oxidation of other atmospheric sulfur species (Logan et al., 1979), while it is emitted anthropogenically from the oxidation of sulfur in combustion from coal, oil, and other sources (Smith et al., 2011; Hidy and Blanchard, 2016). $SO_2$ has direct health effects through the respiratory system with elevated risks for high risk groups (EPA, 2017). Further oxidation of $SO_2$ can form sulfate ($SO_4^{2-}$) which in the form of sulfuric acid ($H_2SO_4$) contributes to acid rain but also contributes to particulate aerosol in the atmosphere (Hidy and Blanchard, 2016). Stratospheric injection of $SO_2$ by volcanoes and subsequent formation of stratospheric aerosol has been proven to have a short-term cooling effect on global climate (Bluth et al., 1997) and therefore is also being considered in some geoengineering scenarios as a possible technique to cool the climate (Rasch et al., 2008; Visioni et al., 2017). Even after decreased $SO_2$ emission by the United States and Europe, continued industrialization in other countries has seen an increase in global $SO_2$ emissions since 2000 (Smith et al., 2011).

There are several well-established measurement techniques for $SO_2$ that have been used in routine air quality monitoring for decades including UV fluorescence (Parrish and Fehsenfeld, 2000) and the pararosaniline wet chemistry technique (West and Gaeke, 1956) which are the two Environmental Protection Agency (EPA) Federal Reference and Equivalent Methods (Gilliam and Hall, 2016). Other techniques include photo-acoustic spectroscopy (Yin et al., 2020), cavity ring-down spectroscopy (Medina et al., 2011), long path differential optical absorption spectroscopy (LP-DOAS) (Stutz and Platt, 1997; Lee et al., 2008),

25 and Multi-Axis Differential Optical Absorption spectroscopy (MAX-DOAS) (Cheng et al., 2019). The LP and MAX-DOAS techniques are not in situ measurements but leverage the spectroscopic signature of $SO_2$ for quantification. The most applied technique is UV fluorescence with several different manufacturers selling instruments for monitoring. One such instrument, the 43i-Trace Level Enhanced from Thermo Electron Corp. (Franklin, MA, USA) has a detection limit of 0.208 ppbv for a 10 second average but can be as low as 0.05 ppbv for a 300 second average with a 1% or 0.2 ppbv precision. UV fluorescence
30 uses pulsed UV light to excite the $SO_2$ molecules which then relax to re-emit light at a longer wavelength. The 43i instrument includes a hydrocarbon kicker to remove most interfering hydrocarbons that also fluoresce when excited with UV light. Known interfering species for fluoresence technique include NO, m-xylene, and $H_2O$.

Broad Band Cavity Enhanced Spectroscopy (BBCEAS) leverages a high finesse optical cavity of a given wavelength to realize long path lengths, similar to LP- and MAX-DOAS but with in situ sampling. Related techniques often add the light
35 source type in front of the acronym (Light Emitting Diode (LED, (Ball et al., 2004)), interband cascade laser (ICL), or Optical Feedback (OF)). BBCEAS and related techniques have been used to measure a number of species including: $NO_2$ (Langridge et al., 2006), $NO_3$ (Venables et al., 2006), $H_2O$, $O_3$ (Thalman and Volkamer, 2010; Axson et al., 2011), glyoxal (Washenfelder et al., 2008), methyl glyoxal (Thalman and Volkamer, 2010), biacetyl (Thalman et al., 2015), IO (Thalman and Volkamer, 2010), $I_2$ (Dixneuf et al., 2009), OIO (Vaughan et al., 2008), ClO, OClO (Dong et al., 2013), ClOOCl (Young et al., 2009), BrO
40 (Hoch et al., 2014), HONO (Gherman et al., 2008), HCHO (Washenfelder et al., 2016), and $O_4$ (Ball et al., 2004; Thalman and Volkamer, 2013) in the UV and visible regions of the spectrum as well as other compounds in the near-IR and IR using related techniques such as Cavity Ring-down Spectroscopy (CRDS) (Brown, 2003), Integrated Cavity Output Spectroscopy (ICOS) (O'Keefe et al., 1999), and Cavity Attenuated Phase Shift Spectroscopy (CAPS) (Kebabian et al., 2005). $SO_2$ was recently measured using OF-CEAS at 4.035 $\mu$m with a detection limit of 130 ppbv (Richard et al., 2016) and CRDS in the UV with a
45 detection limit of 3.5 ppbv in 10 sec (Medina et al., 2011). Previously $SO_2$ was measured by BBCEAS but in the range of 368 - 372 nm but at concentrations of 0.039 - 1% (Chen and Venables, 2011).

Spectroscopic measurement of $SO_2$ in the UV region is based on its highly structured absorption at wavelengths lower than 320 nm. The structured absorption allows for independent quantification of $SO_2$ from other gases that absorb in the same wavelength window including $NO_2$ (Vandaele et al., 1998), $SO_2$ (Bogumil et al., 2003), BrO (Wilmouth et al., 1999),
50 OClO (Bogumil et al., 2003), and many organic molecules with broad absorptions in the UV, acetone being just one example (Gierczak et al., 1998) (Figure 1).

## 2 Experimental

The $SO_2$ cavity instrument consists of the optical cavity, mounted in a 3D-printed cage assembly sitting on top of an instrument control box. Figure 2a shows a schematic of the instrument including standard dilution and supply as well as gas control valves.
55 Figure 2b shows the cage assembly in detail. The BBCEAS instrument consists of a UV LED with a center wavelength of 310 nm (Roithner-Lasertechnik GmbH, DUV310-SD353E) with an output power of 50 mW collimated by a 25 mm f/1 UV lens. The LED was temperature controlled with a Peltier cooler to 10.0±0.1°C. The optical cavity consists of a pair of 2.5 cm
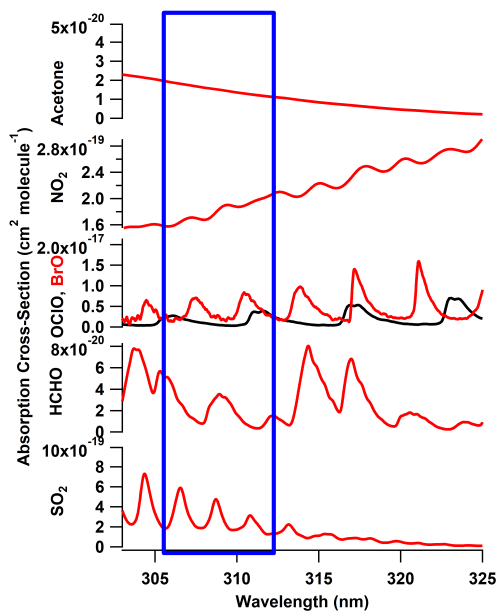
**Figure 1.** Absorption cross-sections of species absorping in the 300 - 320 nm range including, $SO_2$, $NO_2$, BrO, OClO, acetone, and HCHO. The spectral fitting window for the $SO_2$ BBCEAS is shown in blue.
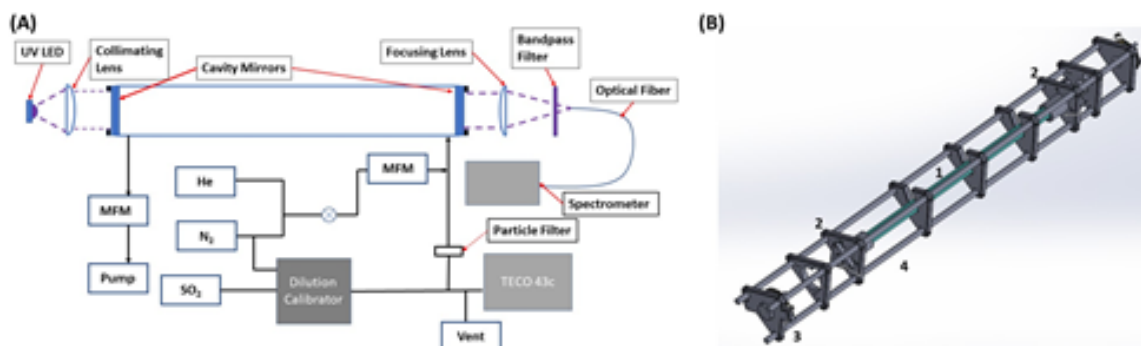
**Figure 2.** Panel A is a schematic of BBCEAS cavity as set up for comparison with the $SO_2$ standard. Panel B: CAD drawing of optical cage assembly. 1:Optical cavity 2: 99.9% Reflective mirrors 3: LED source 4: Cage assembly 5: Kinematic mount to fiber optic

diameter high reflectivity mirrors with a center wavelength of 310 nm, a stated maximum reflectivity of 99.9%, and a radius of curvature of 100 cm (Layertec GmbH). Filtered sample air enters and exits the cavity by the mirrors, utilizing the entire cavity length. The optical cavity consists of a 0.75-inch outer diameter PFA Teflon tube placed between the mirrors. Light exiting the cavity is focused onto an optical fiber (Thorlabs, 6x200 $\mu$m round to linear bundle for the Avantes spectrometer and a 1 mm solid core fiber for the Andor spectrometer) by a 1-inch f/4 lens and filtered by a 12.5mm diameter bandpass filter

(10 nm FWHM, 310 nm, Edmund Optics). The fiber is then directed to the slit of a grating spectrometer. For this work, two

different spectrometers were tested, an Avantes 2048-SPU2 grating spectrometer with a range of 260 – 820 nm and a slit width

65   of 10 $\mu$m, and an Andor DU440-BV Spectrograph with a SR-303i CCD camera cooled by a Peltier cooler to -20°C with a

1200 grooves/mm grating. For the Andor spectrometer the slit was closed until a resolution of 0.26 nm FWHM was achieved,

which provided a sharp well-defined line function. The Avantes spectrometer was not ideal in terms of light efficiency being a

non-cooled detector with increasingly large read-out noise past one second of integration time and a slit width much too small

for the wide range of the detector. The optics are all mounted in an optical cage system constructed of carbon fiber tubes with

70   the braces for the tubes made of 3-D printed parts consisting of either Poly-lactic Acid (PLA) or Acrylic styrene-acrylonitrile

(ASA), printed on an Ender3 (Creality) printer. The material of choice was changed for various structural elements depending

on the structural and design requirement. ASA parts were vapor smoothed to help provide an air tight seal where needed.

Eventually the 3D printed parts were only used for structural support with stainless-steel tubes inserted into the mirror mounts

which sealed via an O-ring to the cavity mirrors. The Teflon tube was held in place between the two stainless steel tubes on each

75   end using a bored-through pipe connection. The reflectivity of the optical cavity was measured using the differential Rayleigh

scattering of He and $N_2$ gas according to the following equation (Thalman and Volkamer, 2010):

$$R(\lambda) = 1 - d_0 \frac{\left(\frac{I_{N_2}(\lambda)}{I_{He}(\lambda)}\right)\epsilon_{Ray}^{N_2}(\lambda) - \epsilon_{Ray}^{He}(\lambda)}{1 - \left(\frac{I_{N_2}(\lambda)}{I_{He}(\lambda)}\right)} \tag{1}$$

Where $d_0$ is the cavity length (95.7 ±0.1 cm), $\epsilon_{Ray}$ is the extinction due to Rayleigh scattering of the respective gasses

(Thalman et al., 2014, 2017) and $I$ is the spectral intensity in the respective gas ($N_2$ or He). The measured reflectivity was

80   found to be 99.85% and the measured reflectivity, effective pathlength and example spectra for $N_2$ and He are given in Figure

3.

The measured concentrations were retrieved by non-linear least squares fitting of the cavity extinction as given by Fiedler

et al. (2003) and Washenfelder et al. (2008):

$$\epsilon(\lambda) = \left(\frac{1 - R(\lambda)}{d_0}\right)\left(\frac{I_0(\lambda) - I(\lambda)}{I(\lambda)}\right) \tag{2}$$

85   where the $\epsilon(\lambda)$ is the wavelength resolved extinction, $R(\lambda)$ is the mirror reflectivity, $d_0$ is the cavity base length, $I_0(\lambda)$ is the

reference spectrum, and $I(\lambda)$ is the measurement spectrum. Previous works with much higher reflectivity mirrors included a

term to account for the Rayleigh scattering of the reference (Washenfelder et al., 2008), this term is omitted for this level of

mirror reflectivity ( 99.8%) and only necessary if the Rayleigh scattering contributes significantly to the extinction in the cavity

(usually at reflectivities > 99.9%).

90   The concentrations of the trace gases of interest was retrieved by non-linear least square fitting in IGOR (Wavemetrics)

by minimizing the error of the following equation with a 3rd degree polynomial enabling a Differential Optical Absorption

Spectroscopy retrieval (Platt and Stutz, 2008):

$$\epsilon(\lambda) = \sigma_{SO_2}(\lambda)[SO_2] + polynomial, \tag{3}$$

Where $\sigma(\lambda)$ is the standard absorption cross section for the given gas and [SO$_2$] is the retrieved concentration of SO$_2$ (Rufus
95  et al., 2003; Bogumil et al., 2003). The absorption cross-sections were convolved to the instrument slit function using the
convolution function in QDOAS (Dankaert et al., 2017). Only SO$_2$ absorption was retrieved as the absorption cross sections
of other gasses are either too small or not in large enough concentrations relative to the sensitivity of the instrument to be
fitted. Cross-sections of SO$_2$ and other possible absorbers are show in Figure 1. Because of the fitted polynomial, the retrieval
is only sensitive to the structured (differential) cross-section and is insensitive to broad changes in the light source shape,
100  aerosol scatter (if no filter was used) and other broad-band absorbers (many organic compounds that interfere with fluorescence
measurements). Fitting was carried out from 305.5 – 312 nm with a 3rd order polynomial and the retrieved concentration was
converted to mixing ratio using the measured temperature and pressure.

### 2.1 Comparison to SO$_2$ standard

Initial testing of the BBCEAS instrument was carried out in comparison to an SO$_2$ standard cylinder (Airgas, 10.14 ppm SO$_2$ in
105  N$_2$) diluted using a dilution calibrator (Environics, model 6103). The diluted standard was supplied to a manifold and sampled
into the BBCEAS through a 47mm PTFE particle filter (Pall) using a pump at 0.8 lpm. The diluted standard was also sampled
by a Thermo 43c SO$_2$ monitor to observe the response of the calibrator.

### 2.2 Noise Evaluation

To evaluate the limit of detection, N$_2$ was continuously flowed through the cavity for several hours with a 1 sec integration
110  time. Spectra were then averaged to a range of total integration times and evaluated with the Beer-Lambert Law (Absorption
= ln(I$_0$/I)) to assess the root mean square noise (RMS). Pure photon counting noise followed the relationship RMS = $1/\sqrt{N}$,
where N is the number of photons collected.

## 3 Results

### 3.1 Comparison to SO$_2$ standard

115  The BBCEAS followed the response of the SO$_2$ concentration delivered by the dilution calibrator linearly. Figure 4 shows
the measured SO$_2$ concentrations with time. Figure 5 shows the fit examples of various concentration levels of SO$_2$ showing
unstructured residuals. The correlation of the standard dilution from the calibrator with the BBCEAS retrieved concentrations
gave a slope of 1.01, an offset of -0.85 ppbv, and an $R^2$ value of 0.9985 (Figure 6). The absence of any structure in the residuals
suggests no systematic error in the fitting routine. The fit residual was improved by 20% at higher concentrations by the use of
120  the Rufus et al. Rufus et al. (2003) rather that the Bogumil et al. Bogumil et al. (2003) cross-section. The minimum fit residual
for the 1 minute average is 3 x 10$^{-8}$ cm$^{-1}$. The variability of the retrieved concentration at each concentration level indicated a
limit of detection of 3.6 ppbv (3-$\sigma$) for a 1-minute acquisition.
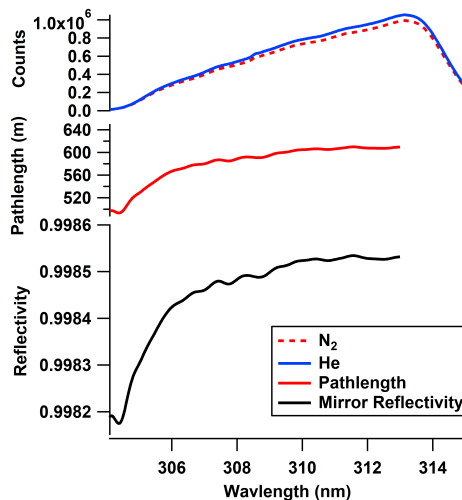
**Figure 3.** Top panel: Signal in the presence of He and $N_2$ gas. Middle Panel: Effective pathlength (1/e) in meters. Bottom Panel: Measured mirror reflectivity in the useable wavelength range.
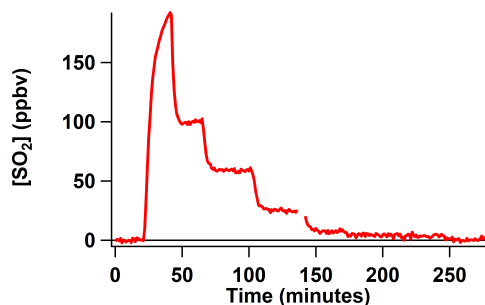
**Figure 4.** : Time series of retrieved $SO_2$ concentrations.

## 3.2 Noise Evaluation

Signal to noise evaluation was carried out on spectra of $N_2$ both with the Andor and Avantes spectrometers. The spectra from the Andor spectrometer were taken from the start and finish of the $SO_2$ comparison tests, allowing for a maximum sampling time of 20 minutes with a single scan integration time of 3 s. The Avantes spectrometer was operated with an integration time of 2 s. The data from the Avantes Spectrometer show a plateau at 3 x $10^{-3}$ RMS and a total integration time of 5 minutes (Figure 7). For the Andor data no plateau is shown for up to 20 minutes of integration time and a minimum RMS of 6.5 x $10^{-4}$.

125
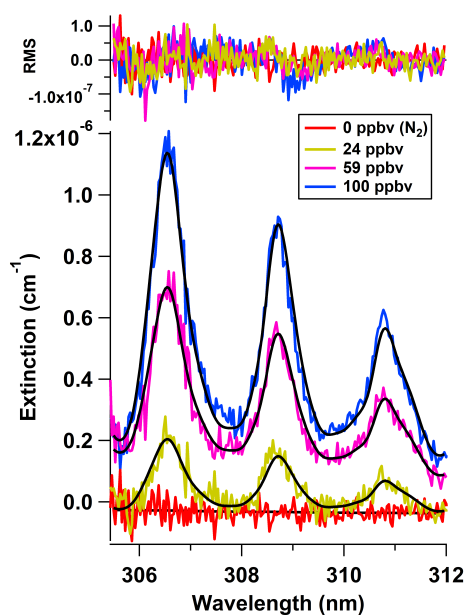
**Figure 5.** : Fitted extinctions of $SO_2$ at mixing ratios of 0, 27, 65, and 112 ppbv with fit residuals shown in the top panel.
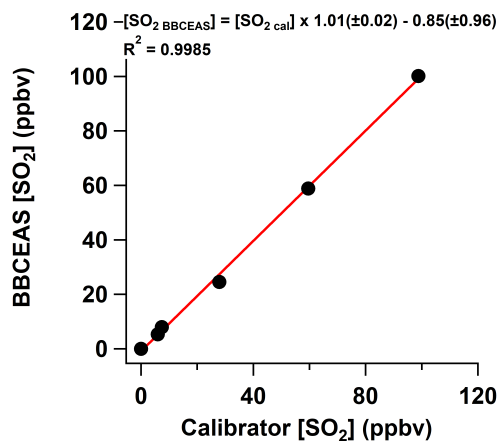
**Figure 6.** Correlation of BBCEAS measured $SO_2$ mixing ratio with the dilution calibrator.

## 4 Conclusions

130   The BBCEAS instrument as currently constructed provides a complimentary technique for the measurement of $SO_2$ with similar limits of detection and linearity over a wide range of $SO_2$ concentrations, like what common commercial instruments for ambient monitoring can provide. In the current configuration the 3-$\sigma$ detection limit is 3.6 ppbv for a 1 minute integration
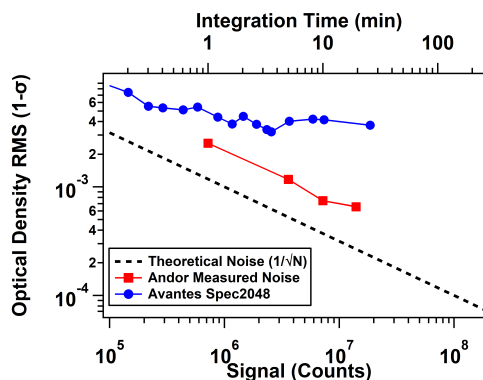
**Figure 7.** Signal to noise evaluationfor both the Andor and Avantes spectrometers evaluated as the 1-$\sigma$ RMS noise. The top and bottom axes correspond to the data for the Andor spectrometer while the Avantes data is only plotted relative to the total signal (bottom axis)

time. The instrument is calibrated with pure gases of $N_2$ and helium, removing the need for standards to be kept in the field for calibration. Known interferences from NO, m-xylene, and $H_2O$ in the instruments utilizing fluorescence detection are avoided

135   using the BBCEAS method.

### 4.1   Improvements to Limit of Detection

Due to the broadened nature of the absorption lines of $SO_2$ (~1 nm FWHM), the instrument resolution of the Andor spectrograph (0.26 nm) was unnecessarily narrow. In initial testing the instrument slit was narrowed to reduce the light coming into the spectrograph so that the integration of a single scan was 3 s with 80% saturation on the chip. The slit was able to be opened

140   wider with the 80% chip saturation occurring at the minimum integration time of 0.1 s. This provides a 30x improvement in the signal. Given that the signal-to-noise improvement in the noise evaluation follows the theoretical relationship for photon counting, the RMS noise would improve to 4 x $10^{-4}$ for a 1 minute integration time, yielding a 3-$\sigma$ limit of detection of 0.6 ppbv in 1 min. This improvement in signal to noise allows for trace level detection of $SO_2$ in the presence of other structured absorbers. The demonstration of workable BBCEAS measurements further in to the UV spectral range with lower reflectivity mirrors

145   allows for measurement of an increasingly large number of molecules by BBCEAS in the UV and visible light ranges. Further development of higher-powered UV LEDs provides enough light to access detection limit ranges of atmospheric importance (Washenfelder et al., 2016). Future development of the BBCEAS instrument could be made to lower the power requirements to a level low enough to allow the instrument to be mounted on a mobile platform such as an Unmanned Aerial System (UAS) for $SO_2$ source identification for larger emitters.

150   *Data availability.*   Data for the experiments and figures are available in the Supplementary Material

*Author contributions.* RT constructed the instrument, performed data analysis and wrote the paper. JCH participated in $SO_2$ comparison tests and contributed to writing the paper.

*Competing interests.* The Authors declare no competing interest.

*Acknowledgements.* This work was supported by the Utah NASA Space Grant Consortium Faculty Research Seed Funding Award.

# References

155   Axson, J. L., Washenfelder, R. A., Kahan, T. F., Young, C. J., Vaida, V., and Brown, S. S.: Absolute ozone absorption cross section in the Huggins Chappuis minimum (350–470 nm) at 296 K, Atmospheric Chemistry and Physics, 11, 11 581–11 590, https://doi.org/10.5194/acp-11-11581-2011, 2011.

Ball, S. M., Langridge, J. M., and Jones, R. L.: Broadband cavity enhanced absorption spectroscopy using light emitting diodes, Chemical
160   Physics Letters, 398, 68–74, https://doi.org/https://doi.org/10.1016/j.cplett.2004.08.144, 2004.

Bluth, G. J. S., Rose, W. I., Sprod, I. E., and Krueger, A. J.: Stratospheric Loading of Sulfur From Explosive Volcanic Eruptions, The Journal of Geology, 105, 671–684, http://www.jstor.org/stable/10.1086/515972, 1997.

Bogumil, K., Orphal, J., Homann, T., Voigt, S., Spietz, P., Fleischmann, O., Vogel, A., Hartmann, M., Kromminga, H., Bovensmann, H., Frerick, J., and Burrows, J.: Measurements of molecular absorption spectra with the SCIAMACHY pre-flight model: instrument charac-
165   terization and reference data for atmospheric remote-sensing in the 230–2380 nm region, Journal of Photochemistry and Photobiology A: Chemistry, 157, 167–184, https://doi.org/https://doi.org/10.1016/S1010-6030(03)00062-5, atmospheric Photochemistry, 2003.

Brown, S. S.: Absorption Spectroscopy in High-Finesse Cavities for Atmospheric Studies, Chemical Reviews, 103, 5219–5238, https://doi.org/10.1021/cr020645c, pMID: 14664649, 2003.

Chen, J. and Venables, D. S.: A broadband optical cavity spectrometer for measuring weak near-ultraviolet absorption spectra of gases,
170   Atmospheric Measurement Techniques, 4, 425–436, https://doi.org/10.5194/amt-4-425-2011, 2011.

Cheng, Y., Wang, S., Zhu, J., Guo, Y., Zhang, R., Liu, Y., Zhang, Y., Yu, Q., Ma, W., and Zhou, B.: Surveillance of SO₂ and NO₂ from ship emissions by MAX-DOAS measurements and the implications regarding fuel sulfur content compliance, Atmospheric Chemistry and Physics, 19, 13 611–13 626, https://doi.org/10.5194/acp-19-13611-2019, 2019.

Dankaert, T., Fayt, C., Roozendael, M. V., Smedt, I. D., Letocart, V., Merlaud, A., and Pinardi, G.: QDOAS Software user manual, Version
175   3.2, http://uv-vis.aeronomie.be/software/QDOAS, accessed: 2021-01-31, 2017.

Dixneuf, S., Ruth, A. A., Vaughan, S., Varma, R. M., and Orphal, J.: The time dependence of molecular iodine emission from Laminaria digitata, Atmospheric Chemistry and Physics, 9, 823–829, https://doi.org/10.5194/acp-9-823-2009, 2009.

Dong, M., Zhao, W., Huang, M., Chen, W., Hu, C., Gu, X., Pei, S., Huang, W., and Zhang, W.: Near-ultraviolet Incoherent Broadband Cavity Enhanced Absorption Spectroscopy for OClO and CH2O in Cl-initiated Photooxidation Experiment, Chinese Journal of Chemical
180   Physics, 26, 133–139, https://doi.org/10.1063/1674-0068/26/02/133-139, 2013.

EPA: Integrated Science Assessment for Sulfur Oxides-Health Criteria, Tech. Rep. EPA-HQ-ORD-2013-0357, U.S. Environmental Protection Agency, Washington, DC, http://www2.epa.gov/isa/integrated-science-assessment-isa-sulfur-dioxide-health-criteria, 2017.

Fiedler, S. E., Hese, A., and Ruth, A. A.: Incoherent broad-band cavity-enhanced absorption spectroscopy, Chemical Physics Letters, 371, 284–294, https://doi.org/https://doi.org/10.1016/S0009-2614(03)00263-X, 2003.

185   Gherman, T., Venables, D. S., Vaughan, S., Orphal, J., and Ruth, A. A.: Incoherent Broadband Cavity-Enhanced Absorption Spectroscopy in the near-Ultraviolet: Application to HONO and NO2, Environmental Science & Technology, 42, 890–895, https://doi.org/10.1021/es0716913, pMID: 18323118, 2008.

Gierczak, T., Burkholder, J. B., Bauerle, S., and Ravishankara, A.: Photochemistry of acetone under tropospheric conditions, Chemical Physics, 231, 229–244, https://doi.org/https://doi.org/10.1016/S0301-0104(98)00006-8, 1998.

190   Gilliam, J. and Hall, E.: Reference and Equivalent Methods Used to Measure National Ambient Air Quality Standards (NAAQS) Criteria Air Pollutants - Volume I, Tech. Rep. EPA/600/R-16/139, U.S. Environmental Protection Agency, Washington, DC, 2016.

Hidy, G. M. and Blanchard, C.: The changing face of lower tropospheric sulfur oxides in the United States, Elementa: Science of the Anthropocene, 4, https://doi.org/10.12952/journal.elementa.000138, 000138, 2016.

Hoch, D. J., Buxmann, J., Sihler, H., Pöhler, D., Zetzsch, C., and Platt, U.: An instrument for measurements of BrO with LED-based Cavity-Enhanced Differential Optical Absorption Spectroscopy, Atmospheric Measurement Techniques, 7, 199–214, https://doi.org/10.5194/amt-7-199-2014, 2014.

Holasek, R. E., Self, S., and Woods, A. W.: Satellite observations and interpretation of the 1991 Mount Pinatubo eruption plumes, Journal of Geophysical Research: Solid Earth, 101, 27 635–27 655, https://doi.org/https://doi.org/10.1029/96JB01179, 1996.

Kebabian, P. L., Herndon, S. C., and Freedman, A.: Detection of Nitrogen Dioxide by Cavity Attenuated Phase Shift Spectroscopy, Analytical Chemistry, 77, 724–728, https://doi.org/10.1021/ac048715y, pMID: 15649079, 2005.

Langridge, J. M., Ball, S. M., and Jones, R. L.: A compact broadband cavity enhanced absorption spectrometer for detection of atmospheric NO2 using light emitting diodes, Analyst, 131, 916–922, https://doi.org/10.1039/B605636A, 2006.

Lee, J., Kim, K.-H., Kim, Y. J., and Lee, J.: Application of a long-path differential optical absorption spectrometer (LP-DOAS) on the measurements of NO$_2$, SO$_2$, O$_3$, and HNO$_2$ in Gwangju, Korea, Journal of Environmental Management, 86, 750–759, https://doi.org/https://doi.org/10.1016/j.jenvman.2006.12.044, 2008.

Logan, J. A., McElroy, M. B., Wofsy, S. C., and Prather, M. J.: Oxidation of CS$_2$ and COS: sources for atmospheric SO$_2$, Nature, 281, 185–188, https://doi.org/10.1038/281185a0, 1979.

Medina, D. S., Liu, Y., Wang, L., and Zhang, J.: Detection of Sulfur Dioxide by Cavity Ring-Down Spectroscopy, Environmental Science & Technology, 45, 1926–1931, https://doi.org/10.1021/es103739r, pMID: 21309509, 2011.

O'Keefe, A., Scherer, J. J., and Paul, J. B.: cw Integrated cavity output spectroscopy, Chemical Physics Letters, 307, 343–349, https://doi.org/https://doi.org/10.1016/S0009-2614(99)00547-3, 1999.

Parrish, D. D. and Fehsenfeld, F. C.: Methods for gas-phase measurements of ozone, ozone precursors and aerosol precursors, Atmospheric Environment, 34, 1921–1957, https://doi.org/https://doi.org/10.1016/S1352-2310(99)00454-9, 2000.

Platt, U. and Stutz, J.: Differential Optical Absorption Spectroscopy (DOAS)—Principles and Applications, vol. 15, Springer, https://doi.org/10.1007/978-3-540-75776-4, 2008.

Rasch, P. J., Tilmes, S., Turco, R. P., Robock, A., Oman, L., Chen, C.-C. J., Stenchikov, G. L., and Garcia, R. R.: An Overview of Geoengineering of Climate Using Stratospheric Sulphate Aerosols, Philosophical Transactions: Mathematical, Physical and Engineering Sciences, 366, 4007–4037, http://www.jstor.org/stable/25197384, 2008.

Richard, L., Ventrillard, I., Chau, G., Jaulin, K., Kerstel, E., and Romanini, D.: Optical-feedback cavity-enhanced absorption spectroscopy with an interband cascade laser: application to SO$_2$ trace analysis, Applied Physics B, 122, https://doi.org/10.1007/s00340-016-6502-0, 2016.

Rufus, J., Stark, G., Smith, P. L., Pickering, J. C., and Thorne, A. P.: High-resolution photoabsorption cross section measurements of SO$_2$, 2: 220 to 325 nm at 295 K, Journal of Geophysical Research: Planets, 108, https://doi.org/https://doi.org/10.1029/2002JE001931, 2003.

Schwartz, S. E.: Both Sides Now, Annals of the New York Academy of Sciences, 502, 83–144, https://doi.org/https://doi.org/10.1111/j.1749-6632.1987.tb37648.x, 1987.

Smith, S. J., van Aardenne, J., Klimont, Z., Andres, R. J., Volke, A., and Delgado Arias, S.: Anthropogenic sulfur dioxide emissions: 1850–2005, Atmospheric Chemistry and Physics, 11, 1101–1116, https://doi.org/10.5194/acp-11-1101-2011, 2011.

Stutz, J. and Platt, U.: Improving long-path differential optical absorption spectroscopy with a quartz-fiber mode mixer, Appl. Opt., 36, 1105–1115, https://doi.org/10.1364/AO.36.001105, 1997.

Thalman, R. and Volkamer, R.: Inherent calibration of a blue LED-CE-DOAS instrument to measure iodine oxide, glyoxal, methyl gly-
oxal, nitrogen dioxide, water vapour and aerosol extinction in open cavity mode, Atmospheric Measurement Techniques, 3, 1797–1814,
https://doi.org/10.5194/amt-3-1797-2010, 2010.

Thalman, R. and Volkamer, R.: Temperature dependent absorption cross-sections of $O_2$–$O_2$ collision pairs between 340 and 630 nm and at
atmospherically relevant pressure, Phys. Chem. Chem. Phys., 15, 15 371–15 381, https://doi.org/10.1039/C3CP50968K, 2013.

Thalman, R., Zarzana, K. J., Tolbert, M. A., and Volkamer, R.: Rayleigh scattering cross-section measurements of nitrogen, argon, oxygen and
air, Journal of Quantitative Spectroscopy and Radiative Transfer, 147, 171–177, https://doi.org/https://doi.org/10.1016/j.jqsrt.2014.05.030,
2014.

Thalman, R., Baeza-Romero, M. T., Ball, S. M., Borrás, E., Daniels, M. J. S., Goodall, I. C. A., Henry, S. B., Karl, T., Keutsch, F. N., Kim,
S., Mak, J., Monks, P. S., Muñoz, A., Orlando, J., Peppe, S., Rickard, A. R., Ródenas, M., Sánchez, P., Seco, R., Su, L., Tyndall, G.,
Vázquez, M., Vera, T., Waxman, E., and Volkamer, R.: Instrument intercomparison of glyoxal, methyl glyoxal and $NO_2$ under simulated
atmospheric conditions, Atmospheric Measurement Techniques, 8, 1835–1862, https://doi.org/10.5194/amt-8-1835-2015, 2015.

Thalman, R., Zarzana, K. J., Tolbert, M. A., and Volkamer, R.: Erratum to "Rayleigh scattering cross-section measurements of nitrogen,
argon, oxygen and air" J Quant Spectrosc Radiat Transf 147 (2014) 171–177, Journal of Quantitative Spectroscopy and Radiative Transfer,
189, 281–282, https://doi.org/https://doi.org/10.1016/j.jqsrt.2016.12.014, 2017.

Vandaele, A., Hermans, C., Simon, P., Carleer, M., Colin, R., Fally, S., Mérienne, M., Jenouvrier, A., and Coquart, B.: Measurements of
the $NO_2$ absorption cross-section from 42 000 cm-1 to 10 000 cm-1 (238–1000 nm) at 220 K and 294 K, Journal of Quantitative Spec-
troscopy and Radiative Transfer, 59, 171–184, https://doi.org/https://doi.org/10.1016/S0022-4073(97)00168-4, atmospheric Spectroscopy
Applications 96, 1998.

Vaughan, S., Gherman, T., Ruth, A. A., and Orphal, J.: Incoherent broad-band cavity-enhanced absorption spectroscopy of the marine
boundary layer species I2, IO and OIO, Phys. Chem. Chem. Phys., 10, 4471–4477, https://doi.org/10.1039/B802618A, 2008.

Venables, D. S., Gherman, T., Orphal, J., Wenger, J. C., and Ruth, A. A.: High Sensitivity in Situ Monitoring of NO3 in an Atmospheric
Simulation Chamber Using Incoherent Broadband Cavity-Enhanced Absorption Spectroscopy, Environmental Science & Technology, 40,
6758–6763, https://doi.org/10.1021/es061076j, pMID: 17144307, 2006.

Visioni, D., Pitari, G., and Aquila, V.: Sulfate geoengineering: a review of the factors controlling the needed injection of sulfur dioxide,
Atmospheric Chemistry and Physics, 17, 3879–3889, https://doi.org/10.5194/acp-17-3879-2017, 2017.

Washenfelder, R. A., Langford, A. O., Fuchs, H., and Brown, S. S.: Measurement of glyoxal using an incoherent broadband cavity enhanced
absorption spectrometer, Atmospheric Chemistry and Physics, 8, 7779–7793, https://doi.org/10.5194/acp-8-7779-2008, 2008.

Washenfelder, R. A., Attwood, A. R., Flores, J. M., Zarzana, K. J., Rudich, Y., and Brown, S. S.: Broadband cavity-enhanced absorption
spectroscopy in the ultraviolet spectral region for measurements of nitrogen dioxide and formaldehyde, Atmospheric Measurement Tech-
niques, 9, 41–52, https://doi.org/10.5194/amt-9-41-2016, 2016.

West, P. W. and Gaeke, G. C.: Fixation of Sulfur Dioxide as Disulfitomercurate (II) and Subsequent Colorimetric Estimation, Analytical
Chemistry, 28, 1816–1819, https://doi.org/10.1021/ac60120a005, 1956.

Wilmouth, D. M., Hanisco, T. F., Donahue, N. M., and Anderson, J. G.: Fourier Transform Ultraviolet Spectroscopy of the A $2\Pi3/2 \longleftarrow$ X
$2\Pi3/2$ Transition of BrO, The Journal of Physical Chemistry A, 103, 8935–8945, https://doi.org/10.1021/jp991651o, 1999.

Yin, X., Wu, H., Dong, L., Li, B., Ma, W., Zhang, L., Yin, W., Xiao, L., Jia, S., and Tittel, F. K.: ppb-Level $SO_2$ Photoacoustic Sensors with
a Suppressed Absorption–Desorption Effect by Using a 7.41 $\mu$m External-Cavity Quantum Cascade Laser, ACS Sensors, 5, 549–556,
https://doi.org/10.1021/acssensors.9b02448, pMID: 31939293, 2020.

Young, I., Whittaker, K., Cox, R., Jones, R., and Pope, F.: Determining the absorption spectrum of ClOOCl using combined UV absorption spectroscopy and broadband cavity enhanced absorption spectroscopy (BBCEAS), AGU Fall Meeting Abstracts, 2009.